



Defect production and accumulation under hydrogen and helium ion irradiation

Jinnan Yu ^{*}, Xinjie Zhao, Wen Zhang, Wen Yang, Fengmin Chu

China Institute of Atomic Energy, PO Box 275-51, Beijing 102413, People's Republic of China

Abstract

The 316L stainless steel (316L SS) is a candidate material for the first wall of a fusion reactor, which will be irradiated with 14 MeV neutrons and escaped ions. This will produce helium and hydrogen in the matrix, which come both from the transmutation production and escaped ions of the plasma. The synergistic action of high-energy cascades and helium induces important damage, such as swelling, blistering and helium embrittlement. The hydrogen combines with the radiation defects to produce dense tiny bubbles (or voids) and substitutes for gaseous impurities (such as soluted oxygen, nitrogen, sulfur and phosphorus) which react with other composites Fe, Cr, Ni and Mo to form new phases, such as Cr_2O_3 , $(\text{CrFe})_2\text{O}_3$, $(\text{Fe}_2\text{C}_2)_{28}\text{N}$, $(\text{CrMo})\text{N}$, $(\text{Fe}_2\text{Mo})_{12}\text{H}$ and $(\text{FeNi})_9\text{S}_8$. These induce mechanical property changes. The hydrogen combined with helium and high energy cascades will induce more serious damage than that of helium alone. To exhibit the synergistic action of helium and hydrogen, the 316L SS specimens were bombarded with helium, hydrogen and mixed ion beam with energy ranging from 27 to 38 keV to a dose of 10^{17} – 8×10^{18} ions/cm² at 573 K. The results indicate that (a) for the helium ion irradiation, the threshold dose for blistering in the energy range 27–100 keV is higher than that for the 1.0 MeV helium ion irradiation. The surface effects play an important role in the blistering. (b) When specimens bombarded with the mixed beam of helium and hydrogen ions of 27 keV reached the same helium dose (6.4×10^{17} He⁺/cm²), the diameter and density of bubble on surface increase at a ratio of the hydrogen to helium increase. The more hydrogen ions implanted, the easier and more serious the blister is. (c) When the kinetic energy of the mixed beam decreases in the range 10–30 keV, the action of hydrogen ions on the blistering appears more evident. It seems that the hydrogen plays an important role in bubble formation and growth. © 1997 Elsevier Science B.V.

1. Introduction

The first wall materials of a fusion reactor are exposed to the 14 MeV neutron irradiation and hydrogen and helium ion bombardment that escaped from the plasma. There is abundant helium and hydrogen atoms in the matrix, which comes from the transmutation production and escaped ions of plasma. The helium, hydrogen and high energy cascades will play an important role in the microstructural evolution. The stainless steel 316L SS is a candidate material for the first wall of a fusion reactor. In this work the effects of helium, hydrogen and high energy cascades in the microstructure evolution are investigated.

The synergistic action of high-energy cascades and helium induces an important damage, such as swelling, blistering and helium embrittlement [1–3]. The hydrogen combines with radiation defects to produce dense tiny bubble (or voids) and substitutes for gaseous impurities (such as soluted oxygen, nitrogen, sulfur and phosphorus) which react with the other components form new phases, such as Cr_2O_3 , $(\text{CrFe})_2\text{O}_3$, $(\text{Fe}_2\text{C}_2)_{28}\text{N}$, $(\text{CrMo})\text{N}$, $(\text{Fe}_2\text{Mo})_{12}\text{H}$ and $(\text{FeNi})_9\text{S}_8$ [1,4]. These induce mechanical property changes.

According the cross-section for (n, α) and (n, p) reactions by 14 MeV neutrons and the content of plasma, the amount of hydrogen in the matrix is much more than that of helium. Hydrogen and helium can combine with the high energy cascades and transmutational impurities to induce more damage than that of helium alone. In order to find out the synergistic action of helium and hydrogen,

^{*} Corresponding author. Tel.: +86-10 6935 7232; fax: +86-10 6935 7048; e-mail: yujn@sun.ihep.ac.cn.

316L SS specimens were bombarded with helium, hydrogen and a mixed ion beam with energies ranging between 27 and 38 keV to a dose of 10^{17} – 8×10^{18} ions/cm² at 573 K. It was a surprise that synergistic effects between hydrogen and helium ion bombardment occur. In order to discriminate these effects, the main characters about the synergistic action of helium with high-energy cascade and hydrogen with radiation defects are reviewed and the experimental investigations about the synergistic action of helium, hydrogen and radiation defects are described here in detail.

2. The synergistic action of helium with high-energy cascades and hydrogen with radiation defects

The synergistic action of high-energy cascades and helium induces major damage, such as swelling, blistering and helium embrittlement. The irradiation experiments were carried out with a Van De Graaf accelerator and the range, vacancy and particle distribution were calculated by TRIM code. Based on the sectioning technology and TEM observation [1], the distribution of bubble size and bubble density with depth were measured to investigate the character of α -particle irradiation on 316L SS and the relationship between swelling and damage dose (DPA) for some helium-content/damage-dose ratios.

The mean bubble size along the depth is shown in Fig. 1. The shapes of mean bubble size–depth curves are

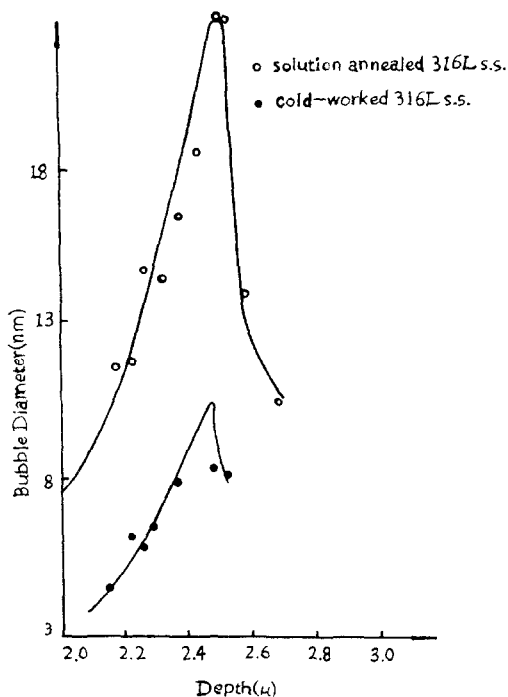


Fig. 1. The mean bubble size (nm) as a function of depth (μm).

similar to those of damage-depth curves. The peak region of mean bubble size approaches the damage peak region (DPR) and its site is at 2.5 μm which is 0.31 μm less than the calculated value of the mean range; therefore the content of helium in this region is not too high. Beyond the mean range, the content of helium is the highest, but the bubble size is small. These facts show the synergistic action of high damage region and helium. In the DPR, the vacancy concentration is the highest, which makes the cascade influence region more wide; the density of bubble nuclei is not too high and the abundant vacancies make the bubble nuclei grow. In addition, the overlap of cascades and their influence regions make the bubbles larger [1]. The result of the synergistic action is that the bubble size is at its largest and the bubble density is lower. In contrast with the DPR, beyond the mean range there is abundant helium and the damage rate is lower. The high helium bubble nucleation and the low vacancy concentration suppress bubble nuclei growth. Therefore, the bubble size is small. This means that the bubble size mainly depends on the vacancy concentration in the region where the helium occurs and the effect of the helium is mainly to form the nucleus of bubbles (or voids). Beyond a depth of 3 μm , which is the calculated maximum range for the helium, there are no bubbles. This shows that the α -particles are all retained in the implantation region and trapped by the displacement damage to form bubble nuclei.

The bubble size distribution at various depths shows that the peak in bubble size distribution shifts to large bubble size with damage dose and the size distribution becomes more wide. The height of the peak decreases with damage dose. These results agree with the theory of bubble nucleation and growth [6].

There is no dislocation in the region where the bubble density and size are large enough. This shows the interaction between dislocations and cascades. Frenkel pairs and helium form bubbles (or voids) and the dislocations are annihilated. Therefore, there are no dislocations in the region along the depth from 1.3 to 2.8 μm .

The microstructure in the cross-section of a specimen irradiated with 1.5 MeV proton to a fluence of 3.7024×10^{19} protons/cm² at 500°C shows that there is a high density of bubbles, which spreads all over the cross-section of the specimen and the diameter of bubble is 2–3 nm. The bubble density for the solid solution and 20% cold-worked specimen at front, middle and rear part has a few differences. The thickness of specimen was 29.4 times the projected range. The proton irradiation not only induced the damage in the region of the projected range, but also in the other regions by hydrogen diffusion along the temperature gradient to other defect sources to form bubbles at 500°C irradiation. A high density of dislocation also appeared in all regions of cross-section of the specimen.

The hydrogen combines with radiation defects to produce dense tiny bubbles (or voids) and substitutes for gaseous impurities (such as soluted oxygen, nitrogen, sul-

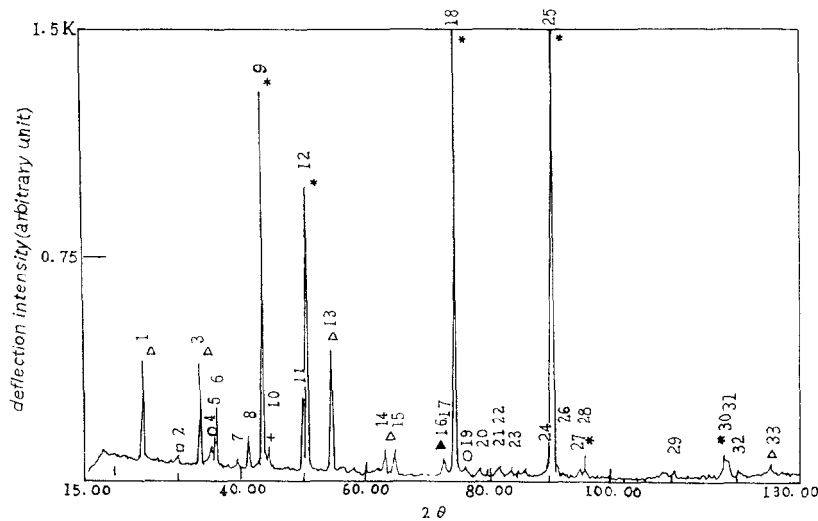


Fig. 2. The X-ray deflection spectrum of the 316L SS specimen irradiated by proton. ★, matrix deflection peak; △, Cr_2O_3 deflection peak; ○, $(\text{CrFe})_2\text{O}_3$ deflection peak; +, $(\text{Fe}_5\text{C}_2)_{28}\text{N}$ deflection peak. ▲ and □ are the $(\text{Fe}_2\text{Mo})_{12}\text{H}$ and $(\text{FeNi})_9\text{S}_8$ deflection peak.

fur and phosphorus) which react with the other components form new phases, such as Cr_2O_3 , $(\text{CrFe})_2\text{O}_3$, $(\text{Fe}_5\text{C}_2)_{28}\text{N}$, $(\text{CrMo})\text{N}$, $(\text{Fe}_2\text{Mo})_{12}\text{H}$ and $(\text{FeNi})_9\text{S}_8$. [1,4], which is shown in Fig. 2. These induce the mechanical property changes. If the hydrogen and helium combine with high-energy cascades and radiation defects, how does the microstructure evolve? Does the synergistic action of hydrogen, helium and cascades occur?

3. The synergistic action of hydrogen, helium and cascades

3.1. Injection facility, target chamber, apparatus and samples

Injection facility: The injector includes duoplasmatron, high voltage sources, lenses, ion mass analyzer and target chamber. The sketch of injector facility is shown in Fig. 3.

The mixed ion beam is generated in duoplasmatron and accelerated by the high voltage source. The beam is fo-

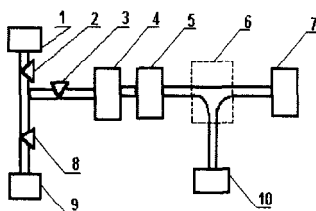


Fig. 3. The sketch of injection facility. (1) He gas source; (2) He-needle valve; (3) needle valve; (4) duoplasmatron; (5) accelerator plus focus lens; (6) mass analyzer magnet; (7) target chamber; (8) H-needle valve; (9) H gas source and (10) mass analyzer apparatus.

cused by a set of lenses. The ratio of helium ions to hydrogen ions in the mixed ion beam is adjusted by the flow rate of helium and hydrogen entering the main pipe and measured by ion mass analyzer. When the ratio of helium ions to hydrogen ions in the beam is selected, the mass analyzer magnet is closed and the mixed ion beam directly bombard the specimen to the assigned dose measured by a digital current integrator and scaler.

The target chamber is shown in Fig. 4. The specimen is shown at 5, which is fixed on the sample holder, 4, by the

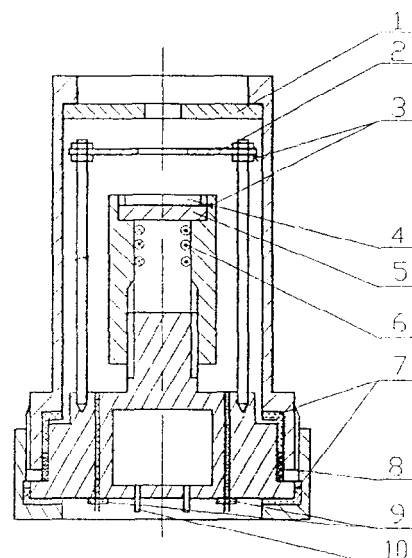


Fig. 4. The irradiation target chamber. (1) Beam limiter; (2) negative voltage ring; (3) thermocouple; (4) sample holder; (5) sample; (6) electrical heater; (7) insulator; (8) sealing ring; (9) sealing wire component and (10) water cooling.

Table 1
Irradiation condition for various specimens

Specimen	Irradiation condition						
	kind of ion	energy (keV)	ratio He/H	ion current $\mu\text{A}/\text{cm}^2$	total dose $\times 10^{17}$ ions/ cm^2	temperature	blistering
01	He ⁺	38	–	30	4	773	rare
02	He ⁺	38	–	30	6.02	773	few
#15	H ⁺	38	–	40	70	773	no
03	He ⁺	27	–	20	4	573	no
#6	He ⁺	27	–	25	6.4	573	few
#1	mixed beam	27	0.40	30	12.0	573	light
#5	mixed beam	27	0.34	30	21.2	573	light
#2	mixed beam	27	0.30	25	21.3	573	light
#4	mixed beam	27	0.20	30	32	573	medium
#3	mixed beam	27	0.12	30	53.3	573	serious

screw ring. The thermocouples, 3, are mounted at the surface of the specimen to measure the specimen surface temperature, whereas other thermocouples are inserted in the negative voltage ring, 2. The electrical heater, 6, is mounted in the sample holder to control the specimen temperature.

The beam limiter, 1, is on the top to let the collimated beam pass through the center hole and bombard the specimen. The negative ring, 2, is to restrain the secondary electron which comes from the bombarding specimen. The wires of thermocouple, electrical heater and negative volt-

age are connected with the sealing wire components, 9. The sample holder is mounted in the container, which is insulated and sealed by the insulator, 7, and sealing ring, 8. There is a water cooling system, 10, on the bottom of the sample holder to protect the temperature of the sealing ring below 373 K.

The diameter of the beam spot is 10 mm. The beam current and fluence at the specimen are measured by a digital current integrator and scaler.

Specimen: The specimens are all of 316L low carbon stainless steel and the thickness of all the specimens is

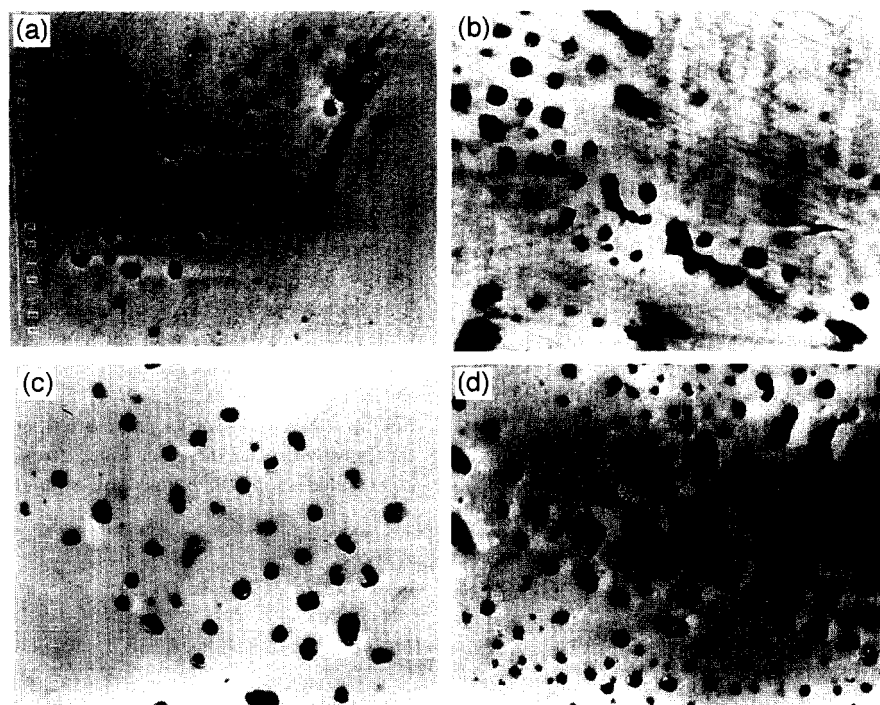


Fig. 5. (a) The flaking on specimen #6 (magnification 4000 \times). (b) The flaking on specimen #2 (magnification 6000 \times). (c) The flaking on specimen #4 (magnification 6000 \times). (d) The flaking on specimen #3 (magnification 6000 \times).

Table 2
The blister for various dose and ratios of helium and hydrogen

Specimen	He dose $\times 10^{17}$	Total dose $\times 10^{17}$	Ratio He/H (%)	Mean diameter (μm)	Density $\times 10^6 \text{ cm}^{-2}$
#6	6.4	6.4	no H	0.562	6.97
#2	6.4	21.3	0.30	0.641	20.7
#4	6.4	32	0.20	0.718	18.3
#3	6.4	53.3	0.12	0.680	38.1

about 0.2 mm. The specimen condition was in solid-solution state and the surface of the specimens was mechanically polished before irradiation to simulate the first wall surface. The surface of the specimens was observed by scanning electron microscopy (SEM) before and after irradiation.

3.2. Experimental results

The irradiation conditions of specimens are shown in Table 1. The helium ion beam with 38 keV bombarded the specimen 01 to $4 \times 10^{17} \text{ He}^+/\text{cm}^2$ at 773 K, it is difficult to find the blister on the surface and occasionally a few bubbles on the surface were found in a tiny area. When the dose is increased to $6.02 \times 10^{17} \text{ He}^+/\text{cm}^2$, there are a few blisters on the surface of specimen 02. When the helium ion beam with 27 keV bombarded the specimen 03 to $4 \times 10^{17} \text{ He}^+/\text{cm}^2$ at 573 K, the results are similar to that for specimen 01 and it is more difficult to find small bubbles on the surface than for specimen 01. The threshold dose of blister with 27 keV helium ion is about $4 \times 10^{17} \text{ He}^+/\text{cm}^2$. When the dose is increased to $6.4 \times 10^{17} \text{ He}^+/\text{cm}^2$, the blister occurs on a few parts of specimen #6 at 573 K. When the mixed beam was adjusted to the ratio of the helium to hydrogen ions at 0.3 and bombarded the specimen #2 at 573 K to $6.4 \times 10^{17} \text{ He}^+/\text{cm}^2$ (total dose $2.13 \times 10^{18} \text{ ion}/\text{cm}^2$), it is easier to find the blister on the specimen and the blistering is light. When the mixed beam with the He/H ratio at 0.2 bombarded the specimen #4 to $6.4 \times 10^{17} \text{ He}^+/\text{cm}^2$ (total dose $3.2 \times 10^{18} \text{ ion}/\text{cm}^2$), the bubbles occurred everywhere on the surface of the specimen and the extent of blistering was fair. When the mixed beam was adjusted to the He/H ratio at 0.12 and specimen #3 was bombarded to $6.4 \times 10^{17} \text{ He}^+/\text{cm}^2$ (total dose $5.33 \times 10^{18} \text{ ion}/\text{cm}^2$), the blistering was intense. These specimens were bombarded by the

mixed beam with three He/H ratios to the same helium ion dose and the blistering increased with hydrogen ion increase.

This show that hydrogen plays an important role in blistering. The pictures of the areas which have bubbles on the surface of specimen #6, #4, #3 are shown in Fig. 5a–d.

The mean diameter and surface density of bubbles were measured by the Videos image analysis system and are shown in Table 2, which indicates that the mean diameter and surface density of bubble increase with the hydrogen content increases.

In contrast, specimen #15 bombarded by hydrogen ions to a dose of $7 \times 10^{18} \text{ ion}/\text{cm}^2$ at 773 K, has no bubble on the surface. This indicates that even hydrogen ions at a very high dose are still not able to induce the blistering.

For the irradiated specimens #1, #2 and #5, the He/H ratios are similar and the helium ion doses are different, their mean diameter and surface density of bubble on the surface are shown in Table 3.

They indicate that the mean diameter and surface density of bubble increase with the helium ion dose increase.

3.3. Discussion

When the helium ions bombarded 316L stainless steel, the threshold dose of blistering decreases with the kinetic energy decrease [2,3]. But as the kinetic energy of helium ions decreases to 170 keV, it seems that the threshold dose of blistering increases with the energy decrease [5]. The present results indicate that the threshold dose of blistering by helium ions with 27 keV is higher than that of the helium ions with 1 MeV. There are three factors to induce the threshold dose increase. First, according to the TRIM code calculation, the range and straggle of helium ions

Table 3
The blister for various helium dose

Specimen	He dose $\times 10^{17}$	Total dose $\times 10^{17}$	Ratio He/H (%)	Mean diameter (μm)	Density $\times 10^6 \text{ cm}^{-2}$
#1	4.8	12.0	0.40	0.596	20.3
#2	6.4	21.3	0.30	0.641	20.7
#5	7.2	21.2	0.34	0.664	21.1

with 27 keV are 114.4 and 47.6 nm, the lateral region and straggle are 50.7 and 56.2 nm and the radial region and its straggle are 79.7 and 37.0 nm. This means that the implantation of helium ions is near the surface and dispersed in a wide region, in which many nuclei of bubbles can be formed and the vacancies produced by helium ions are not enough to cause so much nuclei growth. Otherwise the vacancies near the surface are attracted by the surface and some of them will move to the surface and disappear. The bubble nuclei are more difficult to grow. Thus many tiny bubbles occur in this region and most of them are immobile [6]. According to the gas driven model of blister [7], a larger helium dose is needed to induce blisters. Second, the helium ions with 27 keV bombard the specimens, which have 6.21% backscattered ions. They decrease the implanted quantities of helium and induce the threshold dose increase. Third, the specimen surface was only polished mechanically and had the hardening layer on it, which also induced the increase in the threshold dose.

The implanted region of the hydrogen ions with 27 keV is behind that of the helium ions with a region of overlap. The ion and vacancy distribution in the specimen bombarded by hydrogen and helium ions with 27 keV are shown in Figs. 6 and 7, respectively. The vacancies produced by hydrogen ions in a mixed beam are able to compensate for the loss of vacancies to the surface and are sufficient to fuel bubble growth. The hydrogen enters bubbles to decrease the bubble surface tension, which increases the bubble growth rate. When the bubble size reaches a critical size, the bubble becomes mobile and swallows many tiny bubbles on its path. Due to this bubble growth and coalescence, the bubble becomes large and more easily becomes a blister. This means that greater hydrogen ion implantation supplies more vacancies and hydrogen atoms to prompt the bubble growth and coalescence, the bubble size becomes large and the density of

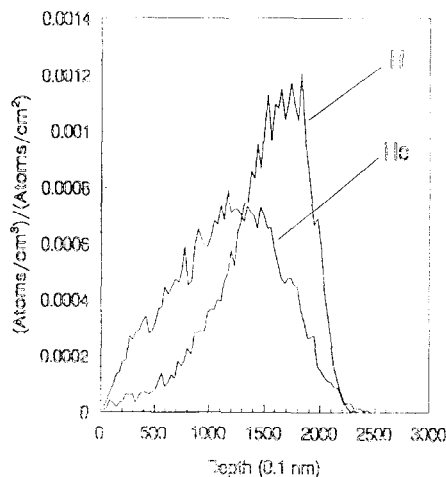


Fig. 6. The ion distribution in the specimen.

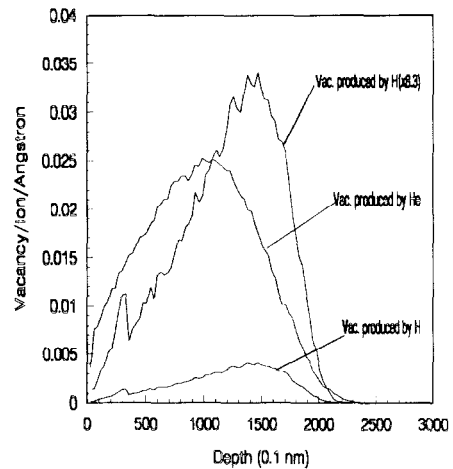


Fig. 7. The vacancy distribution in the specimen.

large bubbles increases and the blistering becomes more intense.

When the kinetic energy of the mixed beam decreases, the range of hydrogen ions is more close to that of helium ions, the hydrogen implanted region will be more overlapped with the helium implanted region and the blistering becomes more intense. Therefore, it is necessary to pay attention to the blister in the energy range 10–30 keV.

4. Summary

(1) The synergistic action of high-energy cascades and helium induces important damage, such as swelling, blistering and helium embrittlement. The threshold dose for blistering in the energy range 10–100 keV is higher than that for the 1.0 MeV helium ion irradiation, the surface effects play an important role in the blistering.

(2) The hydrogen combines with radiation defects to produce dense tiny bubbles (or voids) and substitutes for gaseous impurities (such as soluted oxygen, nitrogen, sulfur and phosphorus) which react with the other components to form new phases, such as Cr_2O_3 , $(\text{CrFe})_2\text{O}_3$, $(\text{Fe}_5\text{C}_2)_{28}\text{N}$, $(\text{CrMo})\text{N}$, $(\text{Fe}_2\text{Mo})_{12}\text{H}$ and $(\text{FeNi})_9\text{S}_8$. The hydrogen implantation does not induce blisters even when the hydrogen dose reaches $9 \times 10^{19} \text{ H/cm}^2$ [2].

(3) The mixed beam of helium and hydrogen ions with the energy 27 keV bombarded the 316L stainless steel to reach the same helium dose, the diameter and density of surface bubble increase at a ratio of the hydrogen to helium increase. The more hydrogen ions implanted, the easier and more serious the blister is. This is because the implanted region of the hydrogen is behind that of helium and with a region at overlap. The vacancies produced by hydrogen ions are able to compensate for the loss of vacancies to the surface and are sufficient to fuel bubble growth and the hydrogen enters bubbles to decrease the

bubble surface tension which increases the bubble growth rate. When the bubble size reaches a critical size, the bubble becomes mobile and swallow many tiny bubbles on its path. Due to this bubble growth and coalescence, the bubble becomes larger and it more easily becomes a blister.

(4) When the kinetic energy of the mixed beam decreases to 10 keV, the implanted region of helium and hydrogen are wider and the range of the hydrogen ion is more close to that of the helium ion, the action of hydrogen ions on the blistering appears more evident. It is necessary to investigate the hydrogen action on the blistering in the energy range 10–30 keV.

References

- [1] J. Yu, Y. Chen, Q. Yang et al., *J. Nucl. Mater.* 191–194 (1992) 728.
- [2] J. Yu, Y. Chen, Y. Shi et al., *J. Nucl. Mater.* 191–194 (1992) 818.
- [3] J. Yu, Y. Chen, Y. Wang et al., *Chin. J. Nucl. Sci. Eng.* 14 (1994) 128.
- [4] X. Zhao, J. Yu, Y. Wang et al., *Chin. J. Nucl. Sci. Eng.* 14 (1994) 58.
- [5] P. Wang, Y. Li, J. Liu et al., *J. Nucl. Mater.* 169 (1989) 167.
- [6] J. Yu, W.F. Sommer, J.N. Bradbury et al., *J. Nucl. Mater.* 227 (1996) 266.
- [7] J.H. Evans, *J. Nucl. Mater.* 68 (1977) 129.